J Neurophysiol 104: 873–884, 2010.
First published June 2, 2010; doi:10.1152/jn.00195.2010.

Cell Specific Dopamine Modulation of the Transient Potassium Current in the Pyloric Network by the Canonical D1 Receptor Signal Transduction Cascade

Hongmei Zhang, Edmund W. Rodgers, Wulf-Dieter C. Krenz, Merry C. Clark, and Deborah J. Baro
Department of Biology, Georgia State University, Atlanta, Georgia

Submitted 19 February 2010; accepted in final form 28 May 2010

Zhang H, Rodgers EW, Krenz WD, Clark MC, Baro DJ. Cell specific dopamine modulation of the transient potassium current in the pyloric network by the canonical D1 receptor signal transduction cascade. *J Neurophysiol* 104: 873–884, 2010. First published June 2, 2010; doi:10.1152/jn.00195.2010. Dopamine (DA) modifies the motor pattern generated by the pyloric network in the stomatogastric ganglion (STG) of the spiny lobster, *Panulirus interruptus*, by directly acting on each of the circuit neurons. The 14 pyloric neurons fall into six cell types, and DA actions are cell type specific. The transient potassium current mediated by shal channels (I_A) is a common target of DA modulation in most cell types. DA shifts the voltage dependence of I_A in opposing directions in pyloric dilator (PD) versus lateral pyloric (LP) neurons. The mechanism(s) underpinning cell-type specific DA modulation of I_A is unknown. DA receptors (DARs) can be classified as type 1 (D1R) or type 2 (D2R). D1Rs and D2Rs are known to increase and decrease intracellular cAMP concentrations, respectively. We hypothesized that the opposing DA effects on PD and LP I_A were due to differences in DAR expression patterns. In the present study, we found that LP expressed somatodendritic D1Rs that were concentrated near synapses but did not express D2Rs. Consistently, DA modulation of LP I_A was mediated by a Gs-adenylyl cyclase-cAMP-protein kinase A pathway. Additionally, we defined antagonists for lobster D1Rs (flupenthixol) and D2Rs (metoclopramide) in a heterologous expression system and showed that DA modulation of LP I_A was blocked by flupenthixol but not by metoclopramide. We previously showed that PD neurons express D2Rs, but not D1Rs, thus supporting the idea that cell specific effects of DA on I_A are due to differences in receptor expression.

INTRODUCTION

The crustacean pyloric network is a powerful model for studying neuromodulation of rhythmic behaviors. All the major cells and their circuit connections are known. Many projection and sensory neurons that modulate the network have been defined (Blitz et al. 2008; Daur et al. 2009; DeLong et al. 2009; Hedrich et al. 2009; Stein et al. 2007), and the modulatory effects of monoamines and peptides on this circuit have been extensively studied (Marder and Bucher 2007; Nusbaum and Beenhakker 2002; Stein 2009).

Pyloric neurons receive both neuromodulatory and -hormonal dopamine (DA) transmissions. A few DA-containing neurons in the two commissural ganglia (COGs) project to the stomatogastric ganglion (STG) via the superior esophageal nerve (Goldstone and Cooke 1971; Kushner and Barker 1983; Kushner and Maynard 1977; Pulver et al. 2003; Sullivan et al. 1977; Tierney et al. 2003) and release DA to pyloric neurons largely in a paracrine fashion (Oginsky et al. 2010). Additionally, the STG resides in a major blood vessel, and the L-cells located in the COGs project to the cardiac ganglion and release neurohormonal DA into the hemolymph (Pulver and Marder 2002; Tierney et al. 2003).

Bath applied DA alters circuit output by differentially modulating pyloric neuron synaptic and intrinsic firing properties (Harris-Warrick et al. 1998). This is partially mediated by DA modulation of several ion channels (Cleland and Selverston 1997; Harris-Warrick et al. 1995a,b, 1998; Johnson et al. 2003a; Kloppenburg et al. 1999, 2000; Peck et al. 2001, 2006). Here we focus on DA modulation of I_A, which helps determine the rate of postinhibitory rebound and spike frequency in pyloric neurons and influences pyloric cycle frequency and phase constancy (Ayali and Harris-Warrick 1998, 1999; Golowasch et al. 1992; Harris-Warrick et al. 1995a,b; Hooper 1997; Johnson et al. 2005;Tierney and Harris-Warrick 1992).

DA targets I_A to differentially alter pyloric neuron activity. For example, in pyloric dilator (PD) neurons bath-applied DA increases I_A maximal conductance and shifts the voltage dependence for activation to more hyperpolarized potentials without altering the voltage dependence for inactivation (Kloppenburg et al. 1999). As a result, the transient (peak) current is increased at all depolarizing membrane potentials where I_A is activated. Further, the window current between the activation and inactivation curves is enlarged, and this increase in the tonic (sustained or steady-state) I_A causes the PD neuron to hyperpolarize. On the other hand, bath applied DA modulates the lateral pyloric (LP) I_A by reducing its maximal conductance and shifting the voltage dependence of both activation and inactivation in the depolarizing direction (Harris-Warrick et al. 1995b). This reduces the transient I_A at all depolarizing potentials and shifts the window current so that the maximal tonic I_A occurs at more depolarized potentials. Ultimately this differential modulation of I_A in PD versus LP neurons contributes to a decrease versus increase in action potential firing and a phase delay versus advancement of neuronal activity, respectively.

The mechanism(s) underpinning this opposing DA modulation of PD and LP I_A is unknown. There are no obvious differences in the ion channels mediating PD and LP I_A. Shal channels mediate I_A and appear to have the same subcellular distribution in both identified cell types such that they are found throughout the somatodendritic compartment and in axon terminals (Baro et al. 1996, 1997, 2000). We therefore hypothesized that differences in DA transduction cascades may underpin the opposing effects of DA on each cell type.

DA acts on several highly conserved DARs that belong to the G-protein-coupled receptor (GPCR) superfamily. In the traditional view, a given type of GPCR signals through one of four classes of G proteins: Gs, Gi/o, Gq/11, and G12/13

Address for reprint requests and other correspondence: D. J. Baro, Dept. of Biology, Georgia State University, P.O. Box 4010, Atlanta GA 30302-4010 (E-mail: dbaro@gsu.edu).

(Cabrera-Vera et al. 2003). All DARs can be classified into two types based on their G protein coupling: D1Rs and D2Rs (Neve et al. 2004). In the canonical pathways, D1Rs couple with Gαs to increase adenylyl cyclase (AC) activity and D2Rs couple with Gαi/o to decrease AC activity, thereby increasing and decreasing cAMP levels, respectively. The change in cAMP concentration will then alter protein kinase A (PKA) activity, which in turn will alter the phosphorylation state of a number of substrates. The two spiny lobster D1Rs, $D_{1\alpha Pan}$ and $D_{1\beta Pan}$, and the single D2R, $D_{2\alpha Pan}$, signal through canonical G-protein-coupled pathways when overexpressed in human embryonic kidney cells (HEK) cells (Clark and Baro 2006, 2007) and in native stomatogastric membrane preparations (Clark et al. 2008). In addition to canonical G-protein-coupled signaling, GPCRs have recently been found to signal through noncanonical pathways that may or may not involve G proteins. We have shown that both types of lobster DARs can signal through evolutionarily conserved, noncanonical pathways. In STG membrane preparations, $D_{1\alpha Pan}$ can couple with Gq to activate phospholipase Cβ (PLCβ) as well as Gs (Clark et al. 2008). It is not clear whether both types of coupling occur in a single neuron and/or whether the distinct cascades alter the same targets. $D_{2\alpha Pan}$ can couple with PLCβ via G$\beta\gamma_{i/o}$ when expressed in HEK cells (Clark and Baro 2007). We have recently shown that PD neurons express D2Rs but not D1Rs (Oginsky et al. 2010). PD DARs are concentrated in perisynaptic regions in the somatodendritic but not axonal compartments. In the present study, we test the hypothesis that DA has opposing effects on PD and LP I_A because LP neurons express D1Rs while PD neurons express D2Rs.

METHODS

Drugs

Drugs were all purchased from Sigma (St. Louis, MO) except Rp-cAMP, tetrodotoxin (TTX), and H-89 (Tocris Bioscience, Bristol, UK). The strategy we used to choose drugs that would block the actions of AC and PKA is as follows: the sites of action for H-89 and Rp cAMP on PKA, and foskolin on AC, were determined from the literature. Using Megalign (DNASTAR), we then aligned these sites in homologues from mammals and invertebrates, including crustaceans. In addition we performed Blast searches with these regions. Together the data suggested that these sites were well conserved across species, a finding also noted in several previous publications. Moreover we only used drugs that were previously shown to work in invertebrates in general and/or specifically in crustaceans.

Animals

California spiny lobsters, *Panulirus interruptus,* were purchased from Don Tomlinson Commercial Fishing (San Diego, CA) and kept in aerated and filtered artificial saltwater.

Dissection and cell identification

Lobsters were cold-anesthetized for ≥30 min and the stomatogastric nervous system (STNS) was dissected as previously described (Bierman and Tobin 2009; Tobin and Bierman 2009). The STNS was pinned in a silicone elastomer (Sylgard)-lined dish and continuously superfused with *Panulirus* (P.) saline, which contained (in mM) 479 NaCl, 12.8 KCl, 13.7 $CaCl_2$, 39 Na_2SO_4, 10 $MgSO_4$, 2 glucose, 4.99 HEPES, and 5 TES; pH 7.4.

Cells were identified using standard intra- and extracellular recording techniques as previously described (Harris-Warrick et al. 1995a,b). Neuronal activity was monitored with intracellular somatic recordings using 20–40 MΩ glass microelectrodes filled with 3 M KCl and Axoclamp 2B or 900A amplifiers (Axon Instruments, Foster City, CA). Extracellular recordings of identified motoneurons were obtained using a differential AC amplifier (A-M Systems, Everett, WA) and stainless steel pin electrodes. Neurons were identified by their distinct waveforms, the timing of their voltage oscillations, and correlation of spikes on the extracellular and intracellular recordings.

Immunohistochemistry (IHC)

The identified LP neuron was filled with a lysine fixable, dextran coupled Texas Red fluorophore that was impermeable to gap junctions (MW 10,000; Molecular Probes), as previously described (Clark et al. 2008). A 1% solution of the fluorophore in 0.2 mol/l KCl was pressure injected (8–20 psi, 200 ms pulse, 0.05 Hz) using an 8–15 MΩ glass microelectrode and a PicoSpritzerIII (General Valve/Parker Hannifin). The fluorophore was injected until the cell became dark purple (typically 15–25 min, depending on the microelectrodes resistance), and the preparation was incubated for 4–24 h at room temperature to allow the fluorophore to diffuse. The preparation was then fixed and DAR protein distributions were determined using whole mount STG preparations in IHC experiments, followed by confocal microscopy. The IHC protocol was as previously described (Baro et al. 2000; Clark et al. 2004). The primary, affinity purified antibodies against the three lobster DARs ($D1_{\alpha Pan}$, $D1_{\beta Pan}$, and $D_{2\alpha Pan}$) and their respective specificities were previously described (Clark et al. 2008; Oginsky et al. 2010). Data were acquired with a LSM510 confocal laser scanning microscope from Carl Zeiss Microimaging (Oberkochen, Germany).

cAMP assays in a heterologous expression system

Receptors were transiently expressed in HEK as previously described (Spitzer et al. 2008a). Cells that overexpressed a given receptor were exposed to DA or DA plus varying concentrations of a given antagonist. The change in cAMP levels induced by DA (10^{-5}M) or DA plus antagonist were measured using an ELISA assay kit (Assay Designs) as previously described (Clark and Baro 2006, 2007; Spitzer et al. 2008a,b). Data were analyzed with Prism (GraphPad) and Excel (Microsoft) software.

TEVC

For two electrode voltage clamp (TEVC), the desheathed stomatogastric nerve (*stn*) and STG were isolated in separate petroleum jelly (Vaseline) wells. The STG was superfused continuously at room temperature with *Panulirus* saline using a Rainin Dynamax peristaltic pump (Rainin). For all experiments, temperature was continuously monitored with a miniature probe in the bath. After cell identification, descending inputs were removed with a sucrose block applied into the well surrounding the *stn* for 1 h. Glutamatergic synaptic inputs were blocked with picrotoxin (10^{-6}M). The known voltage-dependent ion channels except I_A were blocked with bath-applied TTX (10^{-7} M, I_{Na}), TEA (2×10^{-2} M, $I_{K(V)}$ and $I_{K(Ca)}$), CsCl (5×10^{-3} M, I_h) and $CdCl_2$ (2×10^{-4} M, I_{Ca}).

I_A was analyzed as previously described (Baro et al. 1997) using Axoclamp 2B and 900A amplifiers and Clampex 8.2 and 10.2 software (Axon Instruments). The LP neuron was impaled with low resistance (5–9 MΩ) microelectrodes filled with 3 M KCl. Cells were held at −50 mV holding potential between experimental protocols.

The voltage dependence of activation was measured by a series of sweeps in which a hyperpolarizing prepulse to −90 mV for 200 ms was followed by a 500 ms depolarizing test pulse that ranged from −50 to +60 mV with 10 mV increments. Steady-state inactivation was measured with a series of sweeps in which the membrane potential was stepped to a prepulse between −110 and −20 mV with

10 mV increments (200 ms) followed by a constant test pulse to +20 mV (500 ms). Besides the pharmacological isolation described in the preceding text, I_A was further isolated by digital subtraction of the leak conductance. For activation, I_A was evoked by test pulses between −50 and +60 mV from −50 mV holding potential without a negative prepulse. This leaves a relatively linear leak current, which, however, contains a transient component of I_A that is not inactivated at −50 mV. Typically this does not exceed 10% of the peak conductance and was therefore tolerated. These current traces were subtracted from those evoked with negative prepulse. For inactivation, the subtraction protocol contained a depolarizing prepulse to −20 mV before the test pulse to +20 mV.

Data were analyzed with Clampfit v.8.2 and 10.2 (Axon Instruments), Prism v.4 and 5 (Graphpad) and Excel (Microsoft). After digital subtraction, peak currents measured at each voltage step were converted into conductance using the formula $G = I_{peak}/(V - E_K)$, assuming $E_K = -86$ mV (Eisen and Marder 1982). The calculated conductance and the corresponding voltage were then used to construct conductance-voltage plots. Plots were fit with a first-order Boltzmann equation to obtain the maximal conductance (G_{max}), the apparent voltage of half activation ($V_{1/2}$ activation), and voltage of half inactivation ($V_{1/2}$ inactivation).

Many biophysical channel properties are temperature dependent. In preliminary studies, we performed experiments either at room temperature (which did not vary during an experiment and never varied by >3°C across experiments, from 19 to 22°C) or at 16°C (maintained by placing the perfusion tubing in an ice water bath). The results of these studies showed that the DA induced shifts in I_A voltage dependencies were not temperature sensitive. Average shifts were almost exactly the same and not significantly different when measured at room temperature or at 16°C. Therefore for convenience, experiments were performed at room temperature, and all data included in this manuscript were obtained at room temperature.

Drug application

In most experiments, drugs were continuously superfused into the STG well. However, to save on costs, during Rp-cAMP application, perfusion pumps were stopped after the drug was applied to the bath and the bath volume had been replaced at least five times. Pumps were started again for washout. No changes in holding currents or temperature were observed during this process. In all experiments, the concentration of DA was -10^{-5}M, except the Rp-cAMP experiments. To save on costs, DA was reduced to 5×10^{-6} M so that less blocker was required. In some experiments ($n \geq 1$), the order of application was reversed to show that the drug had the same effect regardless of whether or not it was preceded by DA application (e.g., antagonist alone and antagonist +DA applications were before the DA application). We also confirmed that serial applications of DA separated by a 30 min wash had the same effects on LP I_A (i.e., no significant differences in the DA induced shifts produced by DA application 1 vs. 2).

Statistical analyses

Unless otherwise indicated, data are shown as means ± SE. Student's *t*-test were performed with Excel software. One-way (repeated measures) ANOVA was performed with GraphPad Prism software. Tukey's post hoc tests were performed where appropriate. Statistical significance was determined as $P < 0.05$.

RESULTS

D1Rs, but not D2Rs, are expressed in LP neurons

To understand how DA modulates LP I_A, we first defined LP DAR expression. We performed IHC experiments on STG whole mount preparations, each containing a dye-filled LP neuron. Three custom made, affinity purified antibodies, each specific for one of the three lobster DARs, were used in conjunction with confocal microscopy as previously described (Clark et al. 2008; Oginsky et al. 2010). Overlapping 1 μm confocal optical sections throughout the somatodendritic compartment of a given LP neuron were examined for the presence of a given receptor. The data suggested that receptor expression in the somatodendritic compartment was consistent across preparations: $D_{1\alpha Pan}$ and $D_{1\beta Pan}$ receptors were always observed in LP neurons, but $D_{2\alpha Pan}$ receptors were never detected ($n = 5$ for each DAR; Fig. 1).

Similar to our findings for PD D2Rs (Clark et al. 2008; Oginsky et al. 2010), LP D1Rs appeared to be located in somatodendritic endomembrane structures (Fig. 1, *A, B,* and *F*). D1Rs were also detected in primary and higher order neurites (Fig. 1, *C, D,* and *G*). Careful examination of the optical sections showed that receptors were not associated with the plasma membrane in these structures but in endomembrane compartments. Receptors were most highly concentrated in varicosities along, or at the terminals of fine neurites (Fig. 1, *C, E*, *H,* and *I*), which are known to represent synaptic structures (King 1976a,b). $D_{1\alpha Pan}$ and $D_{1\beta Pan}$ receptors often appeared to be in the plasma membrane of synaptic varicosities, as there was no rim of red cytoplasm surrounding receptor immunoreactivity (Fig. 1, *E* and *I*).

Our previous studies suggested that D1Rs may be expressed in glial cells (Oginsky et al. 2010). Figure 1, *A* and *C,* illustrates that $D_{1\beta Pan}$ receptors were highly expressed in the processes of glial and/or other support cells in the STG. It was not clear from our IHC experiments whether or not $D_{1\alpha Pan}$ and $D_{2\alpha Pan}$ receptors were also expressed in glial cells. They are not obviously in the membrane of glial somata as are shal channels (Baro et al. 2000). If these DARs are expressed in glia, they have a punctate distribution and cannot be differentiated from neuronal staining.

LP D1Rs couple with I_A through a Gs-AC-PKA, but not Gq, cascade

We previously showed that $D_{1\alpha Pan}$ and $D_{1\beta Pan}$ couple with Gs, and $D_{1\alpha Pan}$ can also couple with Gq in STNS membrane preparations (Clark et al. 2008). If DA acts exclusively through D1Rs, then DA effects on LP I_A may be mediated by Gs and/or Gq transduction cascades. A pharmacological dissection of the DA induced transduction cascades modulating LP I_A was therefore performed using TEVC.

Consistent with previous reports (Harris-Warrick et al. 1995b), a 10 min bath application of 10^{-5} M DA decreased the LP I_A evoked by a depolarizing test pulse following a hyperpolarizing prepulse to remove all channel inactivation (Fig. 2*A*). First order Boltzmann fits of the conductance voltage relations for activation and inactivation suggested that this decrease was largely the result of reversible DA induced shifts in I_A voltage dependencies to more positive potentials (Fig. 2*B*). Regardless of their initial voltage dependencies, most cells showed similar depolarizing shifts in their apparent voltages of half activation (Fig. 2*C*) and inactivation (*D*). The average shifts were statistically significant for both activation (3.4 ± 0.3 mV, $n = 41$, paired *t*-test, $P < 0.0001$) and inactivation (3.9 ± 0.3 mV, $n = 33$, paired *t*-test, $P < 0.0001$). It is noteworthy that <10% of the cells examined

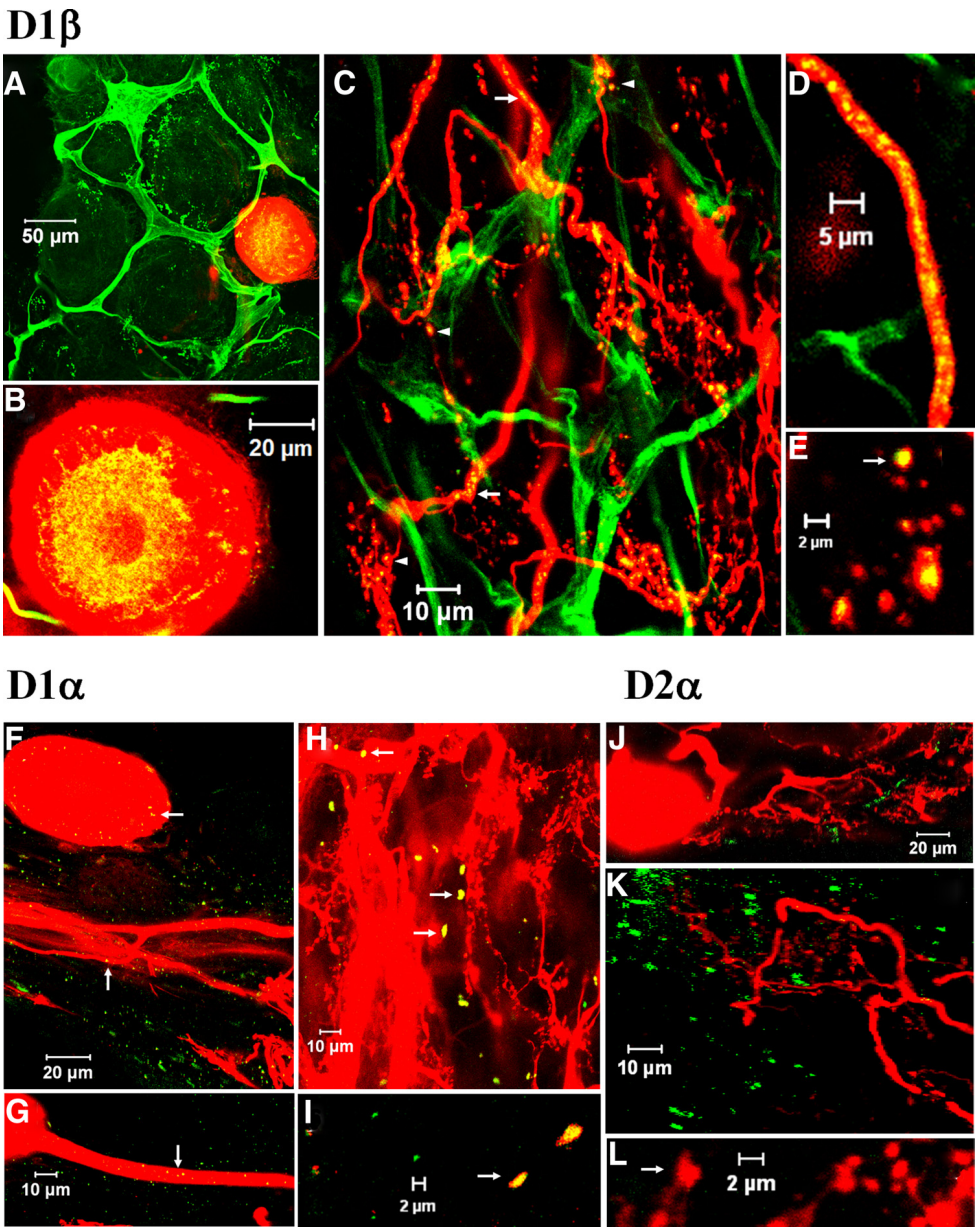

FIG. 1. $D_{1\alpha Pan}$ and $D1_{\beta Pan}$, but not $D_{2\alpha Pan}$ receptors were distributed in the lateral pyloric (LP) somatodendritic compartment. Wholemount stomatogastric ganglion (STG) preparations, each containing a single Texas red filled LP, were stained with anti-$D_{1\beta Pan}$ (*A–E*), anti-$D_{1\alpha Pan}$ (*F–I*), or anti-$D_{2\alpha Pan}$ (*J–L*). $n \geq 5$ wholemount preparations for each receptor type. Yellow staining indicates dopamine receptor (DAR) expression in the LP. Green staining represents DAR expression in unidentified cells. Merged confocal projections were made from serial 1 μm confocal optical slices. *A*: merged, 3 μm confocal projection from a wholemount preparation showing $D_{1\beta Pan}$ receptor expression in LP perinuclear vesicles (yellow puncta) and unidentified cells (green puncta). Green tubular structures surrounding somata suggests $D_{1\beta Pan}$ receptor expression in glial and /or other support cells. *B*: a 3 μm merged confocal projection from the center of the LP soma showing $D_{1\beta Pan}$ receptor expression in the perinuclear vesicles. *C*: a 4 μm merged confocal projection from deep within the synaptic neuropil showing $D_{1\beta Pan}$ receptors in cytoplasmic transport vesicles in higher order neurites (→). ▲, putative synaptic varicosities containing $D_{1\beta Pan}$ receptors. *D*: high magnification 1 μm optical slice showing cytoplasmic transport vesicles in higher order neurite. *E*: high magnification 3–4 μm projection showing a cluster of LP synaptic terminals, some of which contain $D_{1\beta Pan}$ receptors.→, the terminal lacking the red cytoplasmic ring structure. *F–H*: 4 μm merged confocal projections showing $D_{1\alpha Pan}$ receptor expression in the LP soma, primary neurite, higher order neurites and synaptic terminals (→). *I*: high magnification 1 μm optical slice showing the presence of $D_{1\alpha Pan}$ receptors on LP synaptic terminals. →, the terminals lacking a red cytoplasmic ring. *J*: a 37 μm merged confocal projection showing the absence of detectable $D_{2\alpha Pan}$ in the LP soma and primary neurites. Green staining represents $D_{2\alpha Pan}$ receptors in unidentified neurons. *K*: a 4 μm confocal projection from deep within the synaptic neuropil showing the absence of $D_{2\alpha Pan}$ in LP higher order neurites and terminals. *L*: high magnification 1 μm optical slice showing a cluster of LP synaptic terminals lacking $D_{2\alpha Pan}$receptors.

did not respond to DA or responded with a smaller negative shift; however, these data were not excluded from the analyses. As previously reported (Harris-Warrick et al. 1995b), we also observed that DA produced a significant decrease the I_A maximal conductance (Fig. 2*A*), but this effect was not reversible and therefore not considered in this study.

We first tested whether DA shifted the voltage dependence of LP I_A via a Gs cascade. AC converts ATP to cAMP, and Gs can stimulate AC activity. Forskolin directly activates AC in all species by binding to the conserved catalytic core (Yan et al. 1997, 1998; Zhang et al. 1997) (see also METHODS), and this drug has been successfully used to activate AC in several

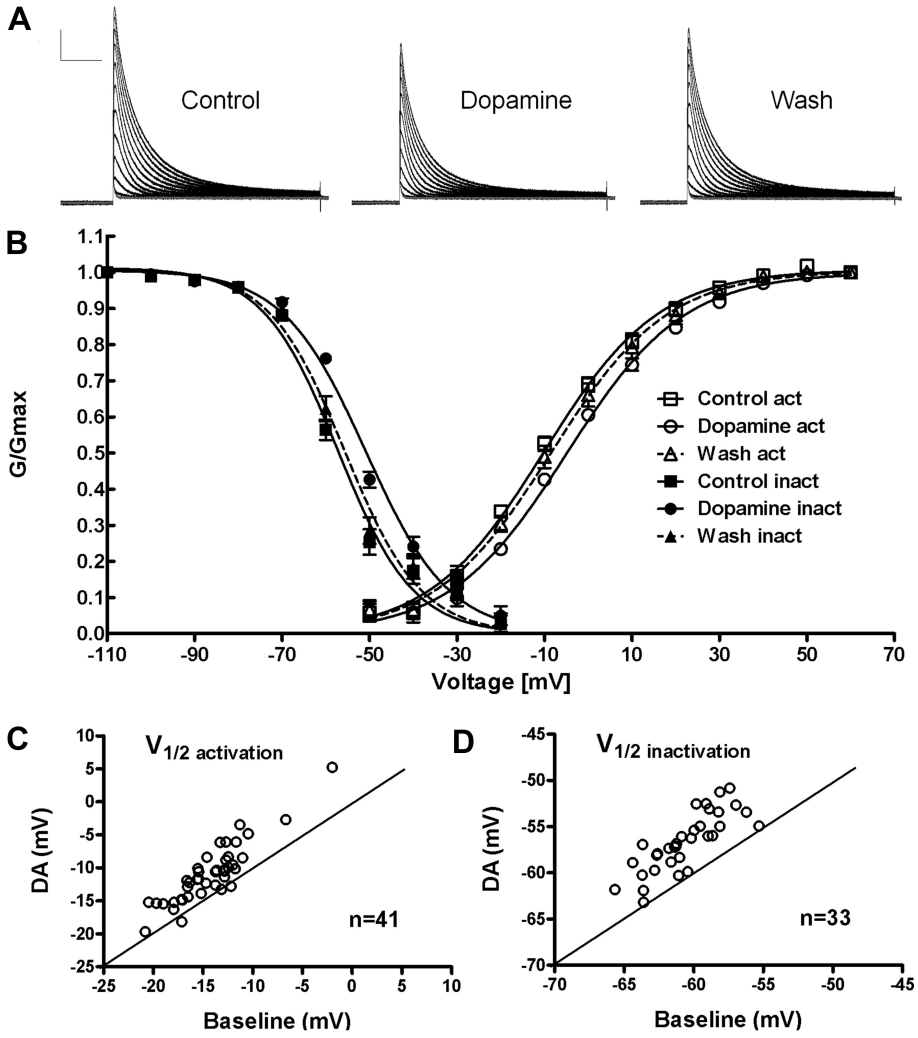

FIG. 2. DA induced positive shifts in the voltage dependence of LP I_A. *A*: TEVC recordings under control conditions, with 10 min bath application of 10^{-5} M DA and after 30 min washout of DA. Current traces were obtained in response to a series of depolarizing test pulses (from −50 to +60 mV in 10 mV increments) following a hyperpolarizing prepulse to −90 mV. All voltage dependent ion channels except I_A were pharmacologically blocked. Scale bars represent 100 ms and 50 nA. *B*: normalized conductance–voltage plots for activation (○, □, △) and inactivation (●, ■, ▲) fit with a 1st-order Boltzmann equation. Plots were obtained under control condition (□, ■), with 10 min 10^{-5} M DA application (○, ●), and after 30 min washout of DA (△, ▲) $n \geq 5$ for each data point. *C* and *D*: preparation-to-preparation variability. ○, the I_A $V_{1/2}$ activation (*C*) and inactivation (*D*) for a single individual in the presence (*y* axis) versus absence (*x* axis) of 10^{-5} M DA. The line indicates unity and points above and below the line indicate that DA shifted the $V_{1/2}$ to more depolarized or hyperpolarized potentials, respectively.

invertebrates including *Drosophila* and crustaceans (Kim and Wu 1996; Klein 1993; Nakatsuji et al. 2009). We asked whether or not forskolin could mimic, and at saturating concentrations occlude, the effects of DA on LP I_A (Fig. 3). A 10 min 10^{-5} M DA application was followed by a 30 min washout, and forskolin (5×10^{-5} M) was applied for 10 min followed by a 10 min application of DA (10^{-5} M) plus forskolin (5×10^{-5} M). LP I_A was recorded at the end of each drug application and wash. Forskolin alone produced depolarizing shifts in the LP I_A $V_{1/2}$ activation (Fig. 3*A*, 6.2 ± 0.8 mV, $n = 5$) and $V_{1/2}$ inactivation (Fig. 3*B*, 3.8 ± 0.7 mV, $n = 5$). These shifts were significantly different from control (ANOVA, $P < 0.01$), but not from the shift induced by DA alone. Thus forskolin mimicked the effects of DA on LP I_A. Moreover, addition of 10^{-5} M DA to preparations that previously received 5×10^{-5} M forskolin did not produce further significant shifts in the voltage dependence (ANOVA, $P > 0.05$). Thus saturating levels of forskolin can occlude the effects of DA on LP I_A. To exclude the possibility that forskolin acted directly on shal channels, rather than on AC, we

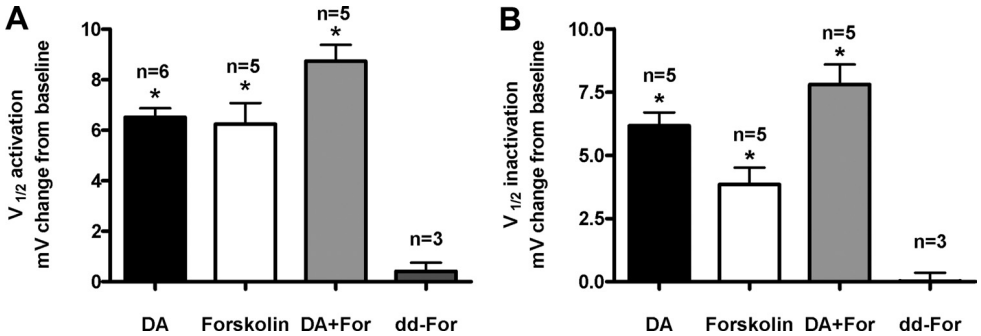

FIG. 3. An adenylyl cyclase (AC) activator mimicked and, at saturating concentrations, largely occluded the effects of DA on LP I_A. I_A was recorded before (baseline) and 10 min after application of 10^{-5} M DA, 5×10^{-5} M forskolin, DA+forskolin, or 5×10^{-5} M dideoxy-forskolin (dd-forskolin). Every preparation received only 1 of the 4 drug treatments. Each drug except dd-forskolin induced a significant and reversible shift in LP I_A $V_{1/2}$ activation (*A*) and inactivation (*B*) relative to baseline. *, significant difference from baseline using 1 way ANOVAs with a Tukey post hoc test.

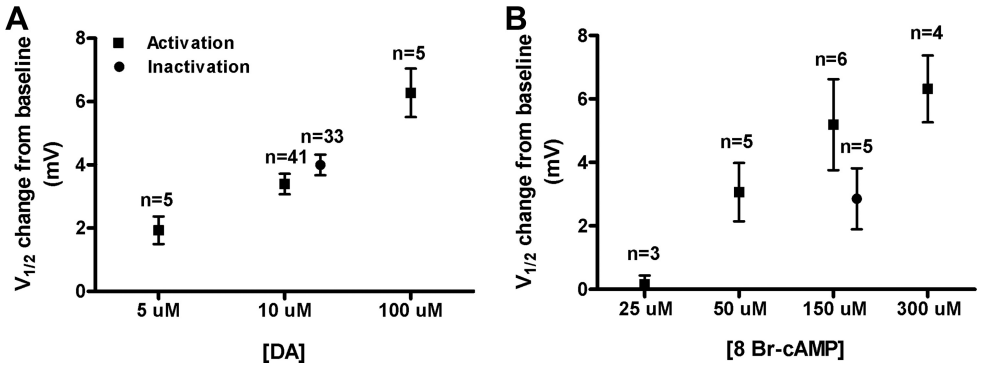

FIG. 4. The cAMP analogue, 8-Br-cAMP, mimicked DA effects on LP I_A. I_A was measured before (baseline) and 10 min after application of DA (*A*) or 8-Br-cAMP (*B*). Every preparation received only 1 dose of either drug. The change from baseline is plotted for I_A $V_{1/2}$ activation (■) inactivation (●).

examined the effect of 1,9-dideoxyforskolin (dd-forskolin), a structural analogue of forskolin that does not activate AC. We found that dd-forskolin had no significant effects on LP I_A ($n = 3$). Taken together, these data suggest that DA shifts the voltage dependence of I_A at least partially through AC.

DA produced dose-dependent shifts in the LP I_A $V_{1/2}$ activation (Fig. 4*A*). If DA signals largely through the Gs cascade, then increasing doses of DA should result in increasing concentrations of cAMP. We therefore asked whether or not cAMP could modulate LP I_A in a dose dependent fashion by bath applying varying concentrations of the membrane permeable cAMP analogue, 8-bromo-cAMP, and measuring the $V_{1/2}$ activation. Note that cAMP is a small second messenger molecule that is not encoded by the genome and that does not vary across species; thus 8-bromo-cAMP will be effective in crustaceans. We found that, like DA, cAMP produced dose-dependent positive shifts in the $V_{1/2}$ activation (Fig. 4*B*). Moreover, similar to the effect of bath applied DA, an increase in the cAMP concentration could also shift the $V_{1/2}$ inactivation to more depolarized membrane potentials (Fig. 4, ●).

PKA is one of the major effectors of cAMP. To test whether PKA was involved in the signaling pathway mediating DA's affect on LP I_A, we examined whether or not the PKA inhibitor, H-89, could block DA's actions. H-89, which has been successfully used in crustaceans (Philipp et al. 2006), inhibits PKA by targeting the ATP binding site (Chijiwa et al. 1990; Engh et al. 1996), which is conserved across species (Gross et al. 1990) (see also METHODS). In these experiments, the preparation was exposed to 10^{-5} M DA for 10 min, followed by a 30 min wash. H-89 (2×10^{-5}M), was then applied for 10 min followed by an application of H-89 plus DA. I_A was recorded prior to DA application, at the end of each drug treatment, and after the 30 min wash. The voltages of half activation and inactivation were determined for each condition, and the change from baseline was plotted in Fig. 5, where baseline is the $V_{1/2}$ prior to drug treatment (DA) or after the wash (H-89, H-89+DA). The data demonstrated that H-89 reversibly inhibited the DA induced shift in $V_{1/2}$ activation (ANOVA, $P < 0.001$, $n = 5$, Fig. 5*A*) and inactivation (ANOVA, $P < 0.001$, $n = 5$, *B*). Because H-89 can also inhibit other kinases, such as PKG, we repeated the experiment with a specific and expensive PKA inhibitor, Rp-cAMP. This drug occupies the cAMP binding site on the regulatory subunit of PKA, thus preventing the holoenzyme from dissociating (Rothermel and Parker Botelho 1988). The cAMP binding site on the regulatory subunit is well conserved across species (Canaves and Taylor 2002) (see also METHODS), and this drug has been used successfully in several arthropods including *Drosophila* and crustaceans (Erxleben et al. 1995; Kuromi and Kidokoro 2000). To save on the cost of the inhibitor in this experiment, the concentration of DA was reduced to 5 μM. Whereas 5 μM DA induced a significant and reversible shift in I_A $V_{1/2}$ activation

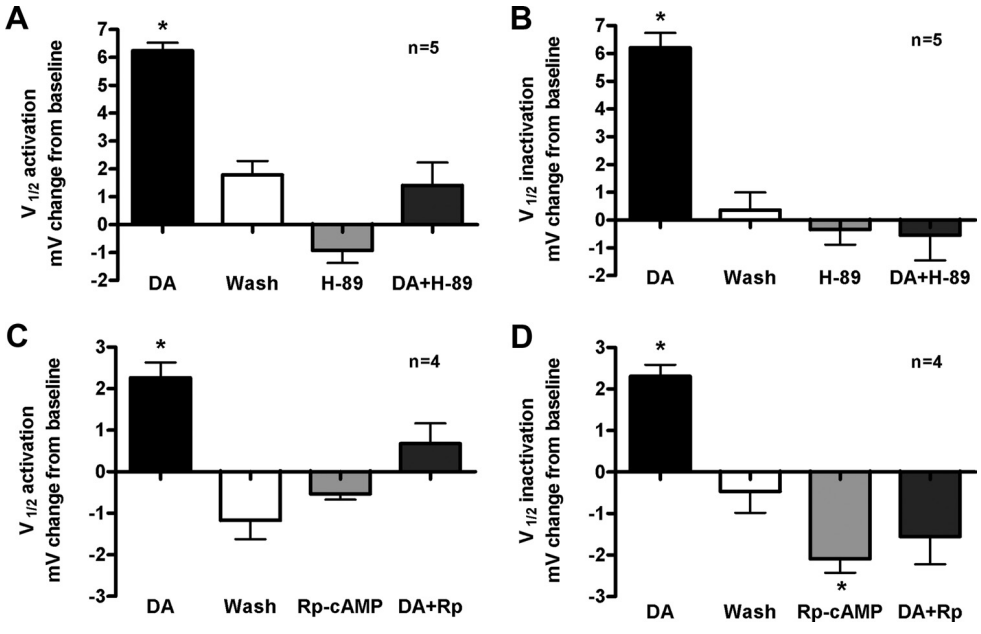

FIG. 5. The protein kinase A (PKA) blockers, H-89 and Rp-cAMP, prevented DA induced changes in LP I_A. I_A was measured before and after a 10 min 10^{-5} M DA application and after a 30 min wash from DA. Measurements from the 1st recording served as baseline for the DA and wash comparisons. After the wash, a 10 min application of 2×10^{-5} M H89 was followed by a 10 min application of DA+H89. I_A was measured at the end of each 10 min application. Measurements from the previous wash served as baseline for H89 comparisons. The change from baseline was plotted for $V_{1/2}$ activation (*A*) and $V_{1/2}$ inactivation (*B*). *C* and *D*: the same experiment was performed except that the concentration of DA was 5×10^{-6} μM and 10^{-3} M Rp-cAMP was substituted for H89. *, significant difference from baseline as determined with 1 way ANOVAs followed by a Tukey pos thoc test.

(ANOVA, $P < 0.001$, $n = 4$, Fig. 5*C*) and inactivation (ANOVA, $P < 0.01$, $n = 4$, Fig. 5*D*), Rp-cAMP blocked this effect. Interestingly, Rp-cAMP itself significantly altered I_A $V_{1/2}$ inactivation (ANOVA, $P < 0.05$, $n = 4$, Fig. 5*D*). This might suggest that PKA constitutively modulates the I_A $V_{1/2}$ inactivation. Indeed, both PKA blockers, H-89 and Rp-cAMP, shifted I_A voltage dependencies in the opposite direction to DA, but in most cases the changes were not statistically significant. Taken together, our data suggest that the Gαs-AC-cAMP-PKA signaling pathway mediates DA modulation of I_A in the LP neuron, consistent with the fact that LP expresses somatodendritic D1Rs but not D2Rs.

As mentioned in the preceding text, $D_{1\alpha Pan}$ receptors also couple with Gq in STNS membrane preparations. PLCβ is the major downstream effector of activated Gαq subunits. The ether lipid analogue ET-18-OCH_3 is a known PLCβ inhibitor (Powis et al. 1992). ET-18-OCH_3 exerts its effects by being incorporated into the plasma membranes of cells (Aroca et al. 2001; Heczkova and Slotte 2006; Powis et al. 1992), but how ET-18-OCH_3 inhibits PLCβ is not clear to date. Nevertheless, ET-18-OCH_3 has been successfully used on invertebrate neurons to inhibit PLCβ (Wong et al. 2007). Using the aforementioned experimental paradigm, we asked whether DA modulation of LP I_A could be blocked by addition of ET-18-OCH_3. Figure 6 illustrates that ET-18-OCH3 did not prevent the DA induced positive shift in LP I_A voltage dependencies, suggesting that DA does not modulates LP I_A through a Gq cascade.

DAR specific antagonists confirm that DA acts on LP I_A through D1Rs

To further confirm that DA modulates LP I_A exclusively through D1Rs, we sought to obtain antagonists specific for lobster D1Rs and D2Rs. It is well established that monoamine receptor pharmacology is not well conserved between vertebrate and invertebrate receptors (Blenau and Baumann 2001; Spitzer et al. 2008a,b; Tierney 2001) because many agonists and antagonists do not bind to evolutionarily conserved amino acids. This is in contrast to the blockers of the transduction cascades that we used (i.e., forskolin, H-89, Rp-cAMP, ET-18-OCH3), which act at functional domains that are evolutionarily conserved. We therefore performed a preliminary screen using a cadre of drugs (Table 1) and found candidate antagonists for lobster D1Rs (flupenthixol) and D2Rs (metoclopramide). The effects of these drugs were characterized in detail using a transient, heterologous expression system and assays for DA induced changes in cAMP concentration in the presence and absence of flupenthixol and metoclopramide. Figure 7 illustrates that, consistent with previous studies (Clark and Baro 2006, 2007), DA altered cAMP levels in both D1R and D2R expressing HEK cells. Flupenthixol, but not metoclopramide, blocked the DA induced increase in cAMP in HEK cells expressing $D_{1\alpha Pan}$ (Fig. 7*A*, $n \geq 3$) and $D_{1\beta Pan}$ receptors (*B*, $n \geq 3$). On the other hand, Fig. 7*C* shows that the DA induced changes in cAMP were prevented by metoclopramide in $D_{2\alpha Pan}$ expressing HEK cells ($n = 3$). If DA acts on LP neurons exclusively through D1Rs, then flupenthixol should block DA modulation of LP I_A, whereas metoclopramide should not. Figure 8 illustrates that this is indeed the case. Using TEVC, we measured the DA induced change in the $V_{1/2}$ activation and $V_{1/2}$ inactivation in LP in the presence and absence of each antagonist. In these experiments, DA (10^{-5} M) was bath applied for 10 min and washed for 30 min; then, 10^{-5} M antagonist was bath applied for 5 min, followed by a 10 min application of antagonist plus DA followed by a 30 min wash. I_A $V_{1/2}$ was measured at the end of each drug application and the wash period. In some cases ($n \geq 1$ for each antagonist), the application order was altered as described in METHODS. We found that 10^{-5} M flupenthixol reversibly blocked the DA induced shift in LP I_A activation from 3.18 ± 0.38 mV ($n = 10$) to 0.27 ± 0.75 mV ($n = 5$) and inactivation from 3.95 ± 0.49 mV ($n = 10$) to 0.81 ± 1.3 mV ($n = 5$). The shifts induced by DA were significantly different from those induced by DA+ flupenthixol (ANOVA, $P < 0.01$). On the other hand, metoclopramide had no significant effect on the DA induced changes in LP I_A. Taken together, the data indicate that DA modulates LP I_A exclusively through D1Rs.

DISCUSSION

DA is known to modulate intrinsic neuronal firing properties and synaptic strengths in a number of systems by acting on a

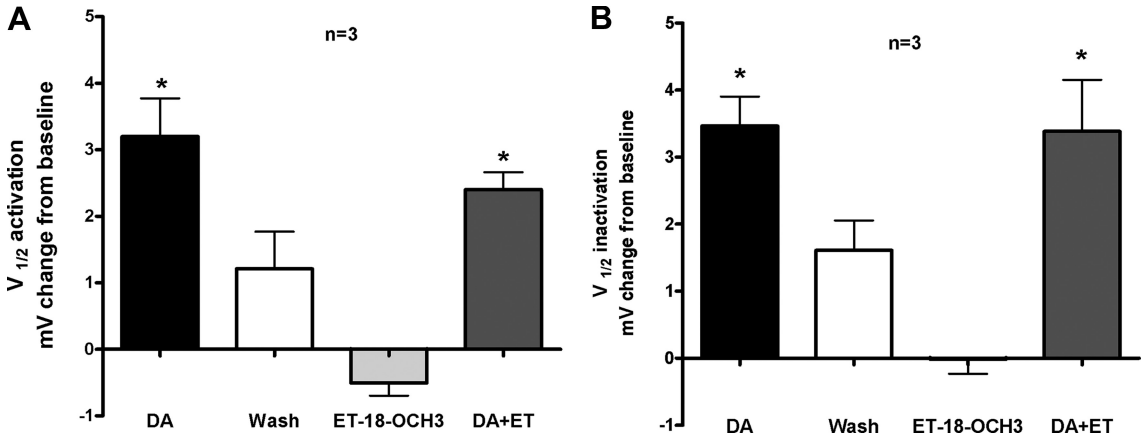

FIG. 6. The PLCβ inhibitor, ET-18-OCH3, did not block DA's effects on LP I_A. I_A was measured before and during a 10 min, 10^{-5} M DA application, after a 30 min washout, and after sequential 10 min applications of 10^{-5} M ET-18-OCH3 and ET-18-OCH3+DA. Measurements from the 1st recording served as baseline for DA and washout comparisons. The washout measurements served as baseline for all subsequent drug applications. The change from baseline was plotted for $V_{1/2}$ activation (*A*) and $V_{1/2}$ inactivation (*B*). *, significant differences from baseline as determined with 1 way ANOVAs followed by Tukey post hoc tests.

TABLE 1. *List of drugs tested to screen DAR antagonists*

Drugs
(−)-Butaclamol
Clozapine
Sulpiride
Haloperidol
Spiperone HCl
Methiothepin mesylate
Metoclopramide
Cyproheptadine HCl
N-R(+)-SCH 23390
Chlorpromazine
(+)-Butaclamol
Domperidone
Eticlopride
Fluphenazine 2HCI
Flupenthixol

Three criteria were used to select an antagonist: ability to block interval pyloric and pyloric dilator I_A; effects on dopamine receptors (DARs) expressed in a heterologous expression system; effects on parental cell lines. Based on these criteria, we chose the best two drugs to examine in detail (flupenthixol and metoclopramide). We have not excluded the possibility that other drugs listed here are effective antagonists for lobster DARs.

plethora of targets in a single cell (Harris-Warrick et al. 1998; Nicola et al. 2000; Surmeier et al. 2007). Whereas the effects of DA on pyloric neurons and network output are well studied, little is known about how the signal is transduced. Here, for the first time, we defined the DA signal transduction cascade operating in an identified pyloric neuron. We found that LP exclusively expressed D1Rs perisynaptically but did not express D2Rs. DA modulation of LP I_A could be pharmacologically blocked by D1R but not D2R antagonists. Further, we demonstrated that LP D1Rs modulated I_A by coupling with the canonical signaling pathway that has been described for D1Rs in all species examined to date: Gs-AC-cAMP-PKA.

Differential effects of DA on LP and PD neurons are due to differences in receptor expression

It was previously shown that DA has opposing effects on two identified cell types of the pyloric motor circuit, LP and PD (Flamm and Harris-Warrick 1986a,b; Harris-Warrick et al. 1995a,b; Johnson et al. 2003a; Kloppenburg et al. 1999, 2000; Peck et al. 2006). DA increases excitability and phase advances LP by increasing calcium currents (I_{Ca}) and a hyperpolarization activated inward current (I_h), while decreasing I_A. DA inhibits PD firing and phase delays neuronal activity by decreasing I_{Ca} and increasing I_A. DA has no effect on PD I_h. Here we demonstrated that the cell specific effects of DA were due to differences in the DA transduction cascade in each cell type. In particular, LP expresses D1Rs and PD expresses D2Rs.

DAR expression was consistent at the protein level for both cell types. Every LP examined expressed somatodendritic $D_{1\alpha Pan}$ and $D_{1\beta Pan}$ but not $D_{2\alpha Pan}$ receptors. Every PD examined expressed D2Rs, but not D1Rs (Oginsky et al. 2010). However, protein levels were not quantified, and receptor number for a given cell type may have varied across preparations. Surface receptors in both cell types appeared to be concentrated in synaptic varicosities within the somatodendritic compartment. These varicosities can represent pre- and/or postsynaptic structures (Oginsky et al. 2010). It is not clear if LP D1Rs are restricted to a subset of synapses as is the case for PD D2Rs (Oginsky et al. 2010).

D1 transduction cascades operate in LP neurons

We showed that DA modulates LP I_A by acting on $D_{1\alpha Pan}$ and/or $D_{1\beta Pan}$ receptors that couple with a Gs-AC-cAMP-PKA pathway. Interestingly, there is no consensus cAMP-dependent phosphorylation site on shal channels (Baro et al. 1996). Shal channels may contain atypical PKA phosphorylation sites (Shi et al. 2007). Alternatively PKA may not act directly on the pore-forming subunit of the A-channel (i.e., shal subunits) but rather target an auxiliary subunit such as KChip (An et al. 2000) or a downstream enzyme (e.g., phosphatase) that then modifies shal subunits.

The fact that DA shifted LP I_A voltage dependencies to more positive potentials through D1R induced increases in cAMP may suggest that DA shifts PD I_A voltage dependencies to more negative potentials via a D2-Gi/o coupled cascade that decreases cAMP and PKA activity. Indeed this is the case in D2R expressing striatal medium spiny neurons (Perez et al. 2006). However, DA may not act simply by reciprocally altering cAMP levels in LP and PD as DARs can act through noncanonical cascades: D2Rs can signal through PLCβ (Clark and Baro 2007; Hernandez-Lopez et al. 2000) and D1Rs can couple with Gq (Clark et al. 2008).

LP D1Rs increase cAMP levels. Interestingly, the literature suggests that cAMP signals can have different spatial attributes. In some cases, the cAMP signal is highly restricted to within one micron of the receptor (Zaccolo and Pozzan 2002), whereas in other cases, the signal can show varying degrees of global spread (Nikolaev et al. 2006; Rich et al. 2001). The type of signal generated does not depend on cell type but on the receptor signaling network (Nikolaev et al. 2006). Global cAMP signals are significantly different from local signals: Global signals are small and sustained, whereas local signals are large and transient (Rich et al. 2001). These distinct types of signals will produce different effects. For example, a global signal may only raise PKA activity slightly causing a small shift in the phosphorylation state of constitutively regulated proteins. On the other hand, a local signal may cause a large change in PKA activity that initiates new cascades by phosphorylating low affinity substrates. Indeed phosphorylation of the low affinity substrate, phosphodiesterase, which degrades cAMP to AMP, may underpin the transient versus sustained nature of the local versus global signal.

In pyloric neurons, surface DARs appeared to be concentrated on synaptic varicosities, which are, themselves, concentrated on the terminals of fine neurites. On the other hand, surface shal channels are localized throughout the somatodendritic compartment including the plasmalemma surrounding the soma and large diameter neurites (Baro et al. 2000). Given the spatial vagary of cAMP signals, and the significantly different character of local and global cAMP signals, this difference in protein distributions raises a very important question: are all shal channels modulated equally? Our current understanding of signal transduction suggests that most likely, they are not. However, the extent to which channels are differentially modulated in each compartment is an important matter for future studies.

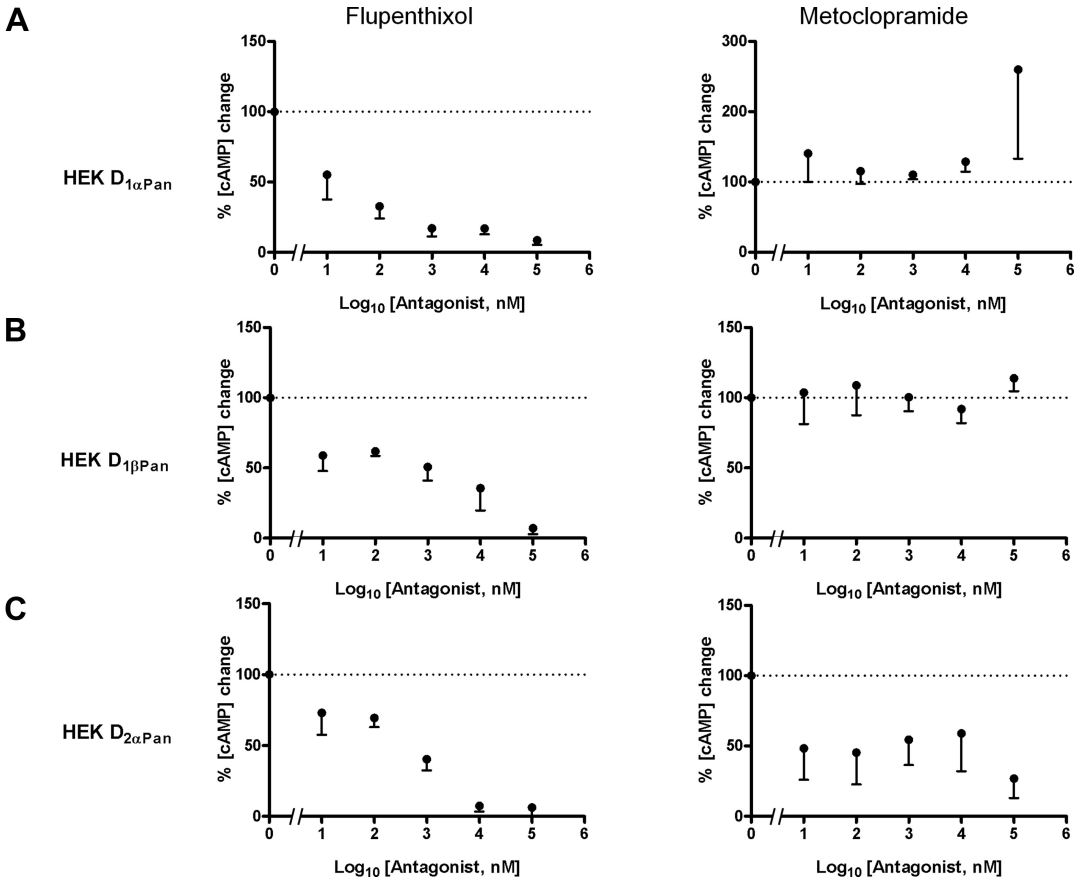

FIG. 7. Dopamine receptor antagonists. cAMP was measured (pmol/mg protein) in cells expressing $D_{1\alpha Pan}$,$D_{1\beta Pan}$, and $D_{2\alpha Pan}$ receptors in the presence of 10^{-5} M DA and increasing concentration of flupenthixol or metoclopramide. Data for a given experiment were normalized to the change in cAMP evoked by DA in the absence of antagonist. The change induced by DA + antagonist are expressed as a percent of the change induced by DA alone (indicated as 100%, - - -). Plots represent the average of ≥3 separate experiments, and a given point was the average of duplicates within each experiment.

Divergent and convergent modulatory systems

Both divergent and convergent modulatory systems exist in the STG. Monoaminergic systems appear to be divergent in three respects. First, a given monoamine can target multiple currents within a cell. For example, DA can alter I_A, I_{Ca}, and I_h in the LP neuron (Harris-Warrick et al. 1995b; Johnson et al. 2003a). Second, a given monoamine can have diverse effects across cell types. For example, DA can increase I_A in the PD neuron, decrease it in the LP, anterior burster (AB), inferior cardiac (IC), and pyloric constrictor (PY) neurons, and have no effect on the ventricular dilator (VD) I_A although the synaptically isolated VD neuron responds to DA and so presumably has DARs (Flamm and Harris-Warrick 1986a,b; Harris-Warrick et al. 1995a,b; Kloppenburg et al. 1999; Peck et al. 2001). Third, each monoamine can alter a given current in different subsets of cells. For example, the effects of DA, serotonin (5-HT) and octopamine (OCT) on I_A were studied in VD, AB, and IC neurons (Peck et al. 2001). All three neurons are known to respond to each modulator in the

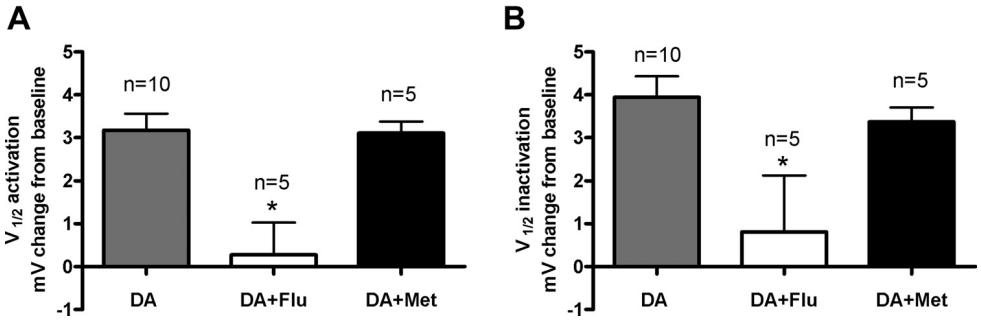

FIG. 8. Flupenthixol but not metoclopramide blocked DA effects on LP I_A. The STG was sequentially exposed to the following treatments: a 10 min, 10^{-5} M DA application, a 30 min wash, a 5 min, 10^{-5} M antagonist application, and a 10 min antagonist + DA application. A given preparation received one antagonist, either flupenthixol (□, $n = 5$) or metoclopramide (■, $n = 5$). LP I_A was recorded at the end of each treatment and immediately before DA application. The change from baseline was plotted for $V_{1/2}$ activation (*A*) and $V_{1/2}$ inactivation (*B*). Measurements from recordings prior to DA application served as the baseline for DA and wash treatments. Measurements from the wash served as baseline for subsequent treatments. *, significant difference from DA alone ($n = 5$) as determined with 1 way ANOVAs followed by Tukey post hoc tests.

intact ganglion and in synaptic isolation, i.e., each cell has receptors for each amine (Flamm and Harris-Warrick 1986a,b). Unlike DA, 5-HT alters I_A only in the IC neuron and OCT has no effect on I_A in AB, IC, or VD neurons. These findings for monoaminergic systems contrast with previously reported convergence in different neuromodulatory systems. Swensen and Marder (2000) demonstrated that five peptides [proctolin, crustacean cardioactive peptide (CCAP), *Cancer borealis* tachykinin related peptide Ia, red pigment-concentrating hormone, and TNRNFLRFamide] and acetylcholine acting at muscarinic receptors consistently altered the same voltage-gated inward current, I_{MI} (Zhao et al. 2010) in all cell types expressing receptors for the aforementioned modulators. However, not all STG neurons expressed all receptors, and the subset of cells that a given convergent modulator acted on varied (Swensen and Marder 2000, 2001). Thus whereas each convergent and divergent modulator can produce a distinct circuit output, they do so by different mechanisms. Convergent modulators will consistently target the same current but in different subsets of cells. On the other hand, each monoamine can differentially target multiple currents within the same cells.

In cases where a given cell expresses receptors for multiple convergent modulators, application of one modulator can occlude the other (Swensen and Marder 2000). This suggests that convergent modulators either signal globally or that the receptors are colocalized if signals are spatially restricted; otherwise, receptor induced changes in the current should be additive. The extent to which divergent monoaminergic modulators can occlude or potentiate one another is not clear. Future experiments using co-application of monoamines should yield valuable information on monoaminergic receptor localization and signaling.

The difference in divergent and convergent systems may be due, in part, to their molecular organization. Monoaminergic systems have multiple GPCRs in invertebrates: DA signals through at least three receptors, 5-HT acts on at least four receptors, and OCT/tyramine bind to eight receptors (Hauser et al. 2006). On the other hand, many of the aforementioned convergent modulators are known to act through a single GPCR in arthropods. In *Drosophila*, multiple studies have revealed that there is a single proctolin receptor (Egerod et al. 2003; Hauser et al. 2006; Johnson et al. 2003b). Similarly, there is one muscarinic receptor (Hauser et al. 2006) and one CCAP receptor (Hauser et al. 2006; Park et al. 2002) although there appear to be two CCAP receptors in the flour beetle (Arakane et al. 2008).

Conclusion

Our present work illuminates the molecular mechanisms underlying DA neuromodulation in an identified pyloric neuron, which is a prerequisite for understanding normal pyloric network function. We have shown that DA modulates LP I_A by acting on $D_{1\alpha Pan}$ and/or $D_{1\beta Pan}$ receptors that couple with a Gs-AC-cAMP-PKA pathway. When considered in light of previous studies, these data not only help to explain the distinct physiological effects of DA on different pyloric cells but also indicate that DAR signal transduction is well conserved across species: DA acts on highly conserved D1Rs and D2Rs in both the crustacean STG and the mammalian striatum, which in turn activate well conserved canonical and noncanonical transduction cascades. The signaling networks activated by homologous DARs in mammals and crustaceans produce similar changes in their target ion channels. Because both the DARs and their ion channel targets can be accurately mapped onto three dimensional reconstructions of identified pyloric neurons, this system can be used for future, broadly applicable studies on the spatial aspects of signal transduction in geometrically complex cells.

ACKNOWLEDGMENTS

We thank K. J. Kent and T. Dever for technical assistance.

GRANTS

H. Zhang was supported by the Georgia State University Molecular Basis of Disease Fellowship. This work was funded by National Institute of Drug Abuse Grant DA024039 to D. J. Baro.

DISCLOSURES

No conflicts of interest, financial or otherwise, are declared by the author(s).

REFERENCES

An WF, Bowlby MR, Betty M, Cao J, Ling HP, Mendoza G, Hinson JW, Mattsson KI, Strassle BW, Trimmer JS, Rhodes KJ. Modulation of A-type potassium channels by a family of calcium sensors. *Nature* 403: 553–556, 2000.

Arakane Y, Li B, Muthukrishnan S, Beeman RW, Kramer KJ, Park Y. Functional analysis of four neuropeptides, EH, ETH, CCAP and bursicon, and their receptors in adult ecdysis behavior of the red flour beetle, *Tribolium castaneum. Mech Dev* 125: 984–995, 2008.

Aroca JD, Sanchez-Pinera P, Corbalan-Garcia S, Conesa-Zamora P, de Godos A, Gomez-Fernandez JC. Correlation between the effect of the anti-neoplastic ether lipid 1-*O*-octadecyl-2-*O*-methyl-glycero-3-phosphocholine on the membrane and the activity of protein kinase Calpha. *Eur J Biochem* 268: 6369–6378, 2001.

Ayali A, Harris-Warrick RM. Interaction of dopamine and cardiac sac modulatory inputs on the pyloric network in the lobster stomatogastric ganglion. *Brain Res* 794: 155–161, 1998.

Ayali A, Harris-Warrick RM. Monoamine control of the pacemaker kernel and cycle frequency in the lobster pyloric network. *J Neurosci* 19: 6712–6722, 1999.

Baro DJ, Ayali A, French L, Scholz NL, Labenia J, Lanning CC, Graubard K, Harris-Warrick RM. Molecular underpinnings of motor pattern generation: differential targeting of shal and shaker in the pyloric motor system. *J Neurosci* 20: 6619–6630, 2000.

Baro DJ, Coniglio LM, Cole CL, Rodriguez HE, Lubell JK, Kim MT, Harris-Warrick RM. Lobster shal: comparison with *Drosophila* shal and native potassium currents in identified neurons. *J Neurosci* 16: 1689–1701, 1996.

Baro DJ, Levini RM, Kim MT, Willms AR, Lanning CC, Rodriguez HE, Harris-Warrick RM. Quantitative single-cell-reverse transcription-PCR demonstrates that A-current magnitude varies as a linear function of shal gene expression in identified stomatogastric neurons. *J Neurosci* 17: 6597–6610, 1997.

Bierman HS, Tobin AE. Gross dissection of the stomach of the lobster, *Homarus americanus. J Vis Exp* May 22(27) pii, 2009.

Blenau W, Baumann A. Molecular and pharmacological properties of insect biogenic amine receptors: lessons from *Drosophila melanogaster* and *Apis mellifera. Arch Insect Biochem Physiol* 48: 13–38, 2001.

Blitz DM, White RS, Saideman SR, Cook A, Christie AE, Nadim F, Nusbaum MP. A newly identified extrinsic input triggers a distinct gastric mill rhythm via activation of modulatory projection neurons. *J Exp Biol* 211: 1000–1011, 2008.

Cabrera-Vera TM, Vanhauwe J, Thomas TO, Medkova M, Preininger A, Mazzoni MR, Hamm HE. Insights into G protein structure, function, and regulation. *Endocr Rev* 24: 765–781, 2003.

Canaves JM, Taylor SS. Classification and phylogenetic analysis of the cAMP-dependent protein kinase regulatory subunit family. *J Mol Evol* 54: 17–29, 2002.

Chijiwa T, Mishima A, Hagiwara M, Sano M, Hayashi K, Inoue T, Naito K, Toshioka T, Hidaka H. Inhibition of forskolin-induced neurite outgrowth and protein phosphorylation by a newly synthesized selective inhibitor of cyclic AMP-dependent protein kinase, *N*-[2-(p-bromocinnamylamino)ethyl]-5-isoquinolinesulfonamide (H-89), of PC12D pheochromocytoma cells. *J Biol Chem* 265: 5267–5272, 1990.

Clark MC, Baro DJ. Molecular cloning and characterization of crustacean type-one dopamine receptors: $D_{1\alpha Pan}$ and $D_{1\beta Pan}$. *Comp Biochem Physiol B Biochem Mol Biol* 143: 294–301, 2006.

Clark MC, Baro DJ. Arthropod D2 receptors positively couple with cAMP through the Gi/o protein family. *Comp Biochem Physiol B Biochem Mol Biol* 146: 9–19, 2007.

Clark MC, Dever TE, Dever JJ, Xu P, Rehder V, Sosa MA, Baro DJ. Arthropod 5-HT2 receptors: a neurohormonal receptor in decapod crustaceans that displays agonist independent activity resulting from an evolutionary alteration to the DRY motif. *J Neurosci* 24: 3421–3435, 2004.

Clark MC, Khan R, Baro DJ. Crustacean dopamine receptors: localization and G protein coupling in the stomatogastric ganglion. *J Neurochem* 104: 1006–1019, 2008.

Cleland TA, Selverston AI. Dopaminergic modulation of inhibitory glutamate receptors in the lobster stomatogastric ganglion. *J Neurophysiol* 78: 3450–3452, 1997.

Daur N, Nadim F, Stein W. Regulation of motor patterns by the central spike-initiation zone of a sensory neuron. *Eur J Neurosci* 30: 808–822, 2009.

DeLong ND, Beenhakker MP, Nusbaum MP. Presynaptic inhibition selectively weakens peptidergic cotransmission in a small motor system. *J Neurophysiol* 102: 3492–3504, 2009.

Egerod K, Reynisson E, Hauser F, Williamson M, Cazzamali G, Grimmelikhuijzen CJ. Molecular identification of the first insect proctolin receptor. *Biochem Biophys Res Commun* 306: 437–442, 2003.

Eisen JS, Marder E. Mechanisms underlying pattern generation in lobster stomatogastric ganglion as determined by selective inactivation of identified neurons. III. Synaptic connections of electrically coupled pyloric neurons. *J Neurophysiol* 48: 1392–1415, 1982.

Engh RA, Girod A, Kinzel V, Huber R, Bossemeyer D. Crystal structures of catalytic subunit of cAMP-dependent protein kinase in complex with isoquinolinesulfonyl protein kinase inhibitors H7, H8, and H89. Structural implications for selectivity. *J Biol Chem* 271: 26157–26164, 1996.

Erxleben CF, deSantis A, Rathmayer W. Effects of proctolin on contractions, membrane resistance, and non-voltage-dependent sarcolemmal ion channels in crustacean muscle fibers. *J Neurosci* 15: 4356–4369, 1995.

Flamm RE, Harris-Warrick RM. Aminergic modulation in lobster stomatogastric ganglion. I. Effects on motor pattern and activity of neurons within the pyloric circuit. *J Neurophysiol* 55: 847–865, 1986a.

Flamm RE, Harris-Warrick RM. Aminergic modulation in lobster stomatogastric ganglion. II. Target neurons of dopamine, octopamine, and serotonin within the pyloric circuit. *J Neurophysiol* 55: 866–881, 1986b.

Goldstone MW, Cooke IM. Histochemical localization of monoamines in the crab central nervous system. *Z Zellforsch Mikrosk Anat* 116: 7–19, 1971.

Golowasch J, Buchholtz F, Epstein IR, Marder E. Contribution of individual ionic currents to activity of a model stomatogastric ganglion neuron. *J Neurophysiol* 67: 341–349, 1992.

Gross RE, Bagchi S, Lu X, Rubin CS. Cloning, characterization, and expression of the gene for the catalytic subunit of cAMP-dependent protein kinase in Caenorhabditis elegans. Identification of highly conserved and unique isoforms generated by alternative splicing. *J Biol Chem* 265: 6896–6907, 1990.

Harris-Warrick RM, Coniglio LM, Barazangi N, Guckenheimer J, Gueron S. Dopamine modulation of transient potassium current evokes phase shifts in a central pattern generator network. *J Neurosci* 15: 342–358, 1995a.

Harris-Warrick RM, Coniglio LM, Levini RM, Gueron S, Guckenheimer J. Dopamine modulation of two subthreshold currents produces phase shifts in activity of an identified motoneuron. *J Neurophysiol* 74: 1404–1420, 1995b.

Harris-Warrick RM, Johnson BR, Peck JH, Kloppenburg P, Ayali A, Skarbinski J. Distributed effects of dopamine modulation in the crustacean pyloric network. *Ann NY Acad Sci* 860: 155–167, 1998.

Hauser F, Cazzamali G, Williamson M, Blenau W, Grimmelikhuijzen CJ. A review of neurohormone GPCRs present in the fruitfly Drosophila melanogaster and the honey bee *Apis mellifera. Prog Neurobiol* 80: 1–19, 2006.

Heczkova B, Slotte JP. Effect of anti-tumor ether lipids on ordered domains in model membranes. *FEBS Lett* 580: 2471–2476, 2006.

Hedrich UB, Smarandache CR, Stein W. Differential activation of projection neurons by two sensory pathways contributes to motor pattern selection. *J Neurophysiol* 102: 2866–2879, 2009.

Hernandez-Lopez S, Tkatch T, Perez-Garci E, Galarraga E, Bargas J, Hamm H, Surmeier DJ. D2 dopamine receptors in striatal medium spiny neurons reduce L-type Ca^{2+} currents and excitability via a novel PLCβ1-IP3-calcineurin-signaling cascade. *J Neurosci* 20: 8987–8995, 2000.

Hooper SL. Phase maintenance in the pyloric pattern of the lobster (*Panulirus interruptus*) stomatogastric ganglion. *J Comput Neurosci* 4: 191–205, 1997.

Johnson BR, Kloppenburg P, Harris-Warrick RM. Dopamine modulation of calcium currents in pyloric neurons of the lobster stomatogastric ganglion. *J Neurophysiol* 90: 631–643, 2003a.

Johnson BR, Schneider LR, Nadim F, Harris-Warrick RM. Dopamine modulation of phasing of activity in a rhythmic motor network: contribution of synaptic and intrinsic modulatory actions. *J Neurophysiol* 94: 3101–3111, 2005.

Johnson EC, Garczynski SF, Park D, Crim JW, Nassel DR, Taghert PH. Identification and characterization of a G protein-coupled receptor for the neuropeptide proctolin in Drosophila melanogaster. *Proc Natl Acad Sci USA* 100: 6198–6203, 2003b.

Kim YT, Wu CF. Reduced growth cone motility in cultured neurons from *Drosophila* memory mutants with a defective cAMP cascade. *J Neurosci* 16: 5593–5602, 1996.

King DG. Organization of crustacean neuropil. I. Patterns of synaptic connections in lobster stomatogastric ganglion. *J Neurocytol* 5: 207–237, 1976a.

King DG. Organization of crustacean neuropil. II. Distribution of synaptic contacts on identified motor neurons in lobster stomatogastric ganglion. *J Neurocytol* 5: 239–266, 1976b.

Klein M. Differential cyclic AMP dependence of facilitation at *Aplysia* sensorimotor synapses as a function of prior stimulation: augmentation versus restoration of transmitter release. *J Neurosci* 13: 3793–3801, 1993.

Kloppenburg P, Levini RM, Harris-Warrick RM. Dopamine modulates two potassium currents and inhibits the intrinsic firing properties of an identified motor neuron in a central pattern generator network. *J Neurophysiol* 81: 29–38, 1999.

Kloppenburg P, Zipfel WR, Webb WW, Harris-Warrick RM. Highly localized Ca^{2+} accumulation revealed by multiphoton microscopy in an identified motoneuron and its modulation by dopamine. *J Neurosci* 20: 2523–2533, 2000.

Kuromi H, Kidokoro Y. Tetanic stimulation recruits vesicles from reserve pool via a cAMP-mediated process in *Drosophila* synapses. *Neuron* 27: 133–143, 2000.

Kushner PD, Barker DL. A neurochemical description of the dopaminergic innervation of the stomatogastric ganglion of the spiny lobster. *J Neurobiol* 14: 17–28, 1983.

Kushner PD, Maynard EA. Localization of monoamine fluorescence in the stomatogastric nervous system of lobsters. *Brain Res* 129: 13–28, 1977.

Marder E, Bucher D. Understanding circuit dynamics using the stomatogastric nervous system of lobsters and crabs. *Annu Rev Physiol* 69: 291–316, 2007.

Nakatsuji T, Lee CY, Watson RD. Crustacean molt-inhibiting hormone: structure, function, and cellular mode of action. *Comp Biochem Physiol A Mol Integr Physiol* 152: 139–148, 2009.

Neve KA, Seamans JK, Trantham-Davidson H. Dopamine receptor signaling. *J Recept Signal Transduct Res* 24: 165–205, 2004.

Nicola SM, Surmeier J, Malenka RC. Dopaminergic modulation of neuronal excitability in the striatum and nucleus accumbens. *Annu Rev Neurosci* 23: 185–215, 2000.

Nikolaev VO, Bunemann M, Schmitteckert E, Lohse MJ, Engelhardt S. Cyclic AMP imaging in adult cardiac myocytes reveals far-reaching beta1-adrenergic but locally confined beta2-adrenergic receptor-mediated signaling. *Circ Res* 99: 1084–1091, 2006.

Nusbaum MP, Beenhakker MP. A small-systems approach to motor pattern generation. *Nature* 417: 343–350, 2002.

Oginsky MF, Rodgers EW, Clark MC, Simmons R, Krenz WD, Baro DJ. D2 receptors receive paracrine neurotransmission and are consistently targeted to a subset of synaptic structures in an identified neuron of the crustacean stomatogastric nervous system. *J Comp Neurol* 518: 255–276, 2010.

Park Y, Kim YJ, Adams ME. Identification of G protein-coupled receptors for *Drosophila* PRXamide peptides, CCAP, corazonin, and AKH supports a

theory of ligand-receptor coevolution. *Proc Natl Acad Sci USA* 99: 11423–11428, 2002.

Peck JH, Gaier E, Stevens E, Repicky S, Harris-Warrick RM. Amine modulation of I_h in a small neural network. *J Neurophysiol* 96: 2931–2940, 2006.

Peck JH, Nakanishi ST, Yaple R, Harris-Warrick RM. Amine modulation of the transient potassium current in identified cells of the lobster stomatogastric ganglion. *J Neurophysiol* 86: 2957–2965, 2001.

Perez MF, White FJ, Hu XT. Dopamine D2 receptor modulation of K^+channel activity regulates excitability of nucleus accumbens neurons at different membrane potentials. *J Neurophysiol* 96: 2217–2228, 2006.

Philipp B, Rogalla N, Kreissl S. The neuropeptide proctolin potentiates contractions and reduces cGMP concentration via a PKC-dependent pathway. *J Exp Biol* 209: 531–540, 2006.

Powis G, Seewald MJ, Gratas C, Melder D, Riebow J, Modest EJ. Selective inhibition of phosphatidylinositol phospholipase C by cytotoxic ether lipid analogues. *Cancer Res* 52: 2835–2840, 1992.

Pulver SR, Marder E. Neuromodulatory complement of the pericardial organs in the embryonic lobster, *Homarus americanus. J Comp Neurol* 451: 79–90, 2002.

Pulver SR, Thirumalai V, Richards KS, Marder E. Dopamine and histamine in the developing stomatogastric system of the lobster *Homarus americanus. J Comp Neurol* 462: 400–414, 2003.

Rich TC, Fagan KA, Tse TE, Schaack J, Cooper DM, Karpen JW. A uniform extracellular stimulus triggers distinct cAMP signals in different compartments of a simple cell. *Proc Natl Acad Sci USA* 98: 13049–13054, 2001.

Rothermel JD, Parker Botelho LH. A mechanistic and kinetic analysis of the interactions of the diastereoisomers of adenosine 3′,5′-(cyclic)phosphorothioate with purified cyclic AMP-dependent protein kinase. *Biochem J* 251: 757–762, 1988.

Shi Y, Wu Z, Cui N, Shi W, Yang Y, Zhang X, Rojas A, Ha BT, Jiang C. PKA phosphorylation of SUR2B subunit underscores vascular K_{ATP} channel activation by beta-adrenergic receptors. *Am J Physiol Regul Integr Comp Physiol* 293: R1205–1214, 2007.

Spitzer N, Cymbalyuk G, Zhang H, Edwards DH, Baro DJ. Serotonin transduction cascades mediate variable changes in pyloric network cycle frequency in response to the same modulatory challenge. *J Neurophysiol* 99: 2844–2863, 2008a.

Spitzer N, Edwards DH, Baro DJ. Conservation of structure, signaling and pharmacology between two serotonin receptor subtypes from decapod crustaceans, Panulirus interruptus and *Procambarus clarkii. J Exp Biol* 211: 92–105, 2008b.

Stein W. Modulation of stomatogastric rhythms. *J Comp Physiol [A]* 195: 989–1009, 2009.

Stein W, DeLong ND, Wood DE, Nusbaum MP. Divergent co-transmitter actions underlie motor pattern activation by a modulatory projection neuron. *Eur J Neurosci* 26: 1148–1165, 2007.

Sullivan RE, Friend BJ, Barker DL. Structure and function of spiny lobster ligamental nerve plexuses: evidence for synthesis, storage, and secretion of biogenic amines. *J Neurobiol* 8: 581–605, 1977.

Surmeier DJ, Ding J, Day M, Wang Z, Shen W. D1 and D2 dopamine-receptor modulation of striatal glutamatergic signaling in striatal medium spiny neurons. *Trends Neurosci* 30: 228–235, 2007.

Swensen AM, Marder E. Modulators with convergent cellular actions elicit distinct circuit outputs. *J Neurosci* 21: 4050–4058, 2001a.

Swensen AM, Marder E. Multiple peptides converge to activate the same voltage-dependent current in a central pattern-generating circuit. *J Neurosci* 20: 6752–6759, 2000.

Tierney AJ. Structure and function of invertebrate 5-HT receptors: a review. *Comp Biochem Physiol A Mol Integr Physiol* 128: 791–804, 2001.

Tierney AJ, Harris-Warrick RM. Physiological role of the transient potassium current in the pyloric circuit of the lobster stomatogastric ganglion. *J Neurophysiol* 67: 599–609, 1992.

Tierney AJ, Kim T, Abrams R. Dopamine in crayfish and other crustaceans: distribution in the central nervous system and physiological functions. *Microsc Res Tech* 60: 325–335, 2003.

Tobin AE, Bierman HS. Homarus americanus stomatogastric nervous system dissection *J Vis Exp* May 28(27) pii 1171, 2009.

Wong R, Fabian L, Forer A, Brill JA. Phospholipase C and myosin light chain kinase inhibition define a common step in actin regulation during cytokinesis. *BMC Cell Biol* 8: 15, 2007.

Yan SZ, Huang ZH, Andrews RK, Tang WJ. Conversion of forskolin-insensitive to forskolin-sensitive (mouse-type IX) adenylyl cyclase. *Mol Pharmacol* 53: 182–187, 1998.

Yan SZ, Huang ZH, Rao VD, Hurley JH, Tang WJ. Three discrete regions of mammalian adenylyl cyclase form a site for Gsalpha activation. *J Biol Chem* 272: 18849–18854, 1997.

Zaccolo M, Pozzan T. Discrete microdomains with high concentration of cAMP in stimulated rat neonatal cardiac myocytes. *Science* 295: 1711–1715, 2002.

Zhang G, Liu Y, Ruoho AE, Hurley JH. Structure of the adenylyl cyclase catalytic core. *Nature* 386: 247–253, 1997.

Zhao S, Golowasch J, Nadim F. Pacemaker neuron and network oscillations depend on a neuromodulator-regulated linear current. *Front Behav Neurosci* 4: 1–9, 2010.